



DESIGN METHODOLOGY FOR THE FIELD ORIENTATION CONTROL OF A NON-LINEAR VECTOR CONTROLLED SINUSOIDAL PERMANENT MAGNET AC MOTOR

P. Ramana¹, M. Surya Kalavathi², K. Alice Mary³ and V. Dinesh Gowri Kumar¹

¹Department of EEE, GMR Institute of Technology Rajam, Srikakulam, AP, India

²Department of EEE, JNTU College of Engineering, Hyderabad, Telangana, India

³Vignan's Institute of Information Technology, Visakhapatnam, Andhra Pradesh, India

E-Mail: pramana.gmrit@gmail.com

ABSTRACT

Nearly all of the electrical power used throughout the world is generated by synchronous machines driven by either hydro or steam turbines or by combustion engines. Synchronous Machine is generally dedicated to high power due to the fact that they have a controllable power factor and a higher efficiency than the induction motor of corresponding rating. In recent years different control schemes using synchronous motors operating from static power converter have been a real competitor to both DC and Induction Motor drives, especially in high power, low speed range. Among them field oriented control employing vector control strategies has become quite popular in recent years. A disadvantage of the scheme when applied to synchronous motor drive is that the motor always operates at a lagging power factor. In this work a generalized design strategy is suggested for speed control loop of an inverter fed synchronous motor drive, in which, its inherent flexibility to generate the same torque for different combinations of currents is exploited. The closed loop system for the Permanent Magnet AC Motor is simulated using MATLAB and the performance figures of some typical cases such as unity power factor control, torque angle control and internal angle control are obtained.

Keywords: permanent magnet AC motor, field oriented control, unity power factor control, internal angle control.

1. INTRODUCTION

Permanent Magnet Synchronous Motors are receiving an increasing amount of attention for drive applications because of their high torque to inertia ratio, superior power density and higher efficiency than that of an induction motor with the same ratings due to no stator power dedicated to the magnetic field production. They are also well adapted, to drive fast dynamic loads. Permanent Magnet Synchronous Motor (PMSM) is increasingly applied in several areas such as Traction, Hybrid Electric Vehicles, Robotics, Aerospace technology etc. In PMSM, field excitation is obtained by mounting permanent magnets on the rotor. This eliminates DC source, losses associated with the field winding and frequent maintenance associated with slip rings and brushes in a wound field synchronous motor. But the power factor cannot be controlled because the field excitation cannot be changed. These motors are usually designed to operate at unity power factor at full load. While projecting type machine has a uniform air gap, the inset and interior types have essentially salient pole construction. The power and torque expressions of salient pole motors are applicable for PMSM also [1].

PMSM is now commonly known as Permanent Magnet AC (PMAC) Motor. They are classified based on the nature of voltage induced in the stator as sinusoidally excited and trapezoidally excited; in the former, induced voltage has a sinusoidal waveform and in the later, induced voltage has trapezoidal waveform. A sinusoidal PMAC motor has distributed winding similar to wound field synchronous motor in the stator. Rotor poles are so shaped that the voltage induced in a stator phase has a sinusoidal

waveform. The speed of PMAC Motor is controlled by feeding them from variable frequency voltages/currents. They are operated in self-control mode. Rotor position sensors are employed for operation in self-control mode. Alternately induced voltage can be used to achieve self-control. Different inverter/converter circuits for PMAC motors using power transistors are employed. The current trend is to use MOSFET for low voltage and low power applications and IGBT for others. The self-controlled variable frequency drives employing, a Sinusoidal PMAC Motors are now called as "Permanent Magnet AC Motor Drives" and a trapezoidal PMAC Motors are now called "Brushless DC Motor Drives". Since the voltages induced in the stator phases of a Sinusoidal PMAC Motors are sinusoidal ideally, the three stator phases must be supplied with variable frequency sinusoidal voltages or currents with a phase difference of 120° between them. Behavior of such a motor from a variable frequency voltage source is described vastly [3].

From the Norton's equivalent of the synchronous motor equivalent circuit [3] of Figure-2(a)

$$\bar{I}_f = \frac{\bar{E}}{jX_s} = \frac{E}{X_s} \angle -(\delta = 90^\circ) \quad (1)$$

$$\bar{I}_m = \bar{I}_s + \bar{I}_f \quad (2)$$

The phasor diagram of the motor with I_s (or i_{phase}) as a reference phasor is shown in Fig. 2(b). The mechanical power developed is



$$P_m = 3EI_s \cos(\delta = \frac{\pi}{2}) \quad (3)$$

Substituting for E from eqn. (1) gives

$$P_m = 3X_s I_s \sin \delta \quad (4)$$

Now

$$T = \frac{P_m}{\omega_{ms}} = KI_s \sin \delta \quad (5)$$

$$\text{Where } K = \frac{3X_s}{\omega_{ms}} = \text{constant}$$

For $\delta = \pm 90^\circ$, $T = \pm KI_f I_s = \pm K_T I_s$, Hence torque is proportional to I_s . For a given value of I_s , maximum torque is obtained when $\delta = \pi/2$, phasor diagram for $\delta = \pi/2$ is shown in Figure-2(c). In this condition, the motor is said to operate with unity internal power factor because I_s is in phase with E. The motor itself has a lagging power factor. It is desirable to obtain maximum torque per unit of stator current, therefore this is the preferred operating condition. Similarly in braking operation, maximum torque per unit of stator current is obtained when

$\delta = \pi/2$, hence this is the preferred operating condition for braking operation. The condition $\delta = \pi/2$ is obtained by reversing stator current I_s . It should be noted that δ is the angle between the rotating fields produced by the stator and rotor and the maximum torque is obtained when the axis of two fields make an angle of $\pm \pi/2$.

In case of flux weakening, there are applications which require speed control in wide range. In wound field motors, the operation up to the base speed is obtained by varying both voltage and frequency. The speed control above the base speed is obtained by reducing the air-gap flux so that motor terminal voltage remains at the rated value as frequency is increased. In Figure-2(c), air-gap flux can be reduced by reducing I_m . In a wound field machine this can be achieved by reducing I_f by reducing field current. This cannot be done in a permanent magnet machine. However, I_m for a given I_s can be progressively reduced by increasing δ with speed, as shown in the phasor diagram of Figure-2(d). At $\delta = 90^\circ$, I_s is in quadrature with I_f , for $\delta > 90^\circ$ I_s can be resolved into two components, one in quadrature with I_f and another in phase opposition to I_f which causes reduction in I_m and air-gap flux. Over the years different methods of closed loop control have been employed for improving the stability and dynamic response of the variable speed (synchronous motor) drive fed from static devices either in open loop mode or in self-control mode involving stator voltage or current control, torque angle control, power factor control and field oriented control [4].

Control system design for inverter-fed drives used the classical transfer function approach for single-input single-output systems, proportional cum-integral (PI) controllers were designed for individual control loops [2]. The proposed controller is represented in the conventional two-loop structure for the motor drive. The outer loop is

the speed controller, the output of which is the reference value of the torque, T_e^* from this value, the reference values of the current i.e., i_{qs}^* and i_{ds}^* are computed for a desired internal angle, ψ and desired torque angle, δ . This gives flexibility in choosing the power factor of the motor from lagging to leading values including unity. The field oriented control can also be obtained as a special case, by setting the power factor angle to be equal to the torque angle, resulting in complete decoupling between the armature flux and the field flux, thus, producing a DC motor like behavior. In this sense, the proposed control scheme is more general than conventional field oriented control.

2. MODELING OF SINUSOIDAL PMAC MOTOR

The Sinusoidal PMAC Motors are similar to the salient pole motors, except that there is no filed winding and the field is provided instead by mounting permanent magnets in the rotor. The excitation voltage cannot be varied. The elimination of field coil, DC Supply and slip rings reduces the motor loss and complexity. These motors, also known as 'Brushless motors' are finding increasing applications in robots and machine tools [6].

The voltage equations for the permanent magnet motor in rotor reference frame are

$$v_{qs} = r_a i_{qs} + l_{qs} p i_{qs} + l_{aq} p i_{qr} + \omega_r l_{ds} i_{ds} + \omega_r l_{ad} i_{dr} + \omega_r \Psi \quad (6)$$

$$v_{ds} = r_a i_{ds} + l_{ds} p i_{ds} + l_{ad} p i_{dr} - \omega_r l_{qs} i_{qs} - \omega_r l_{aq} i_{qr} \quad (7)$$

$$v_{qr} = r_{qr} i_{qr} + l_{qr} p i_{qr} + l_{aq} p i_{qs} \quad (8)$$

$$v_{dr} = r_{dr} i_{dr} + l_{dr} p i_{dr} + l_{ad} p i_{ds} \quad (9)$$

Where, $\Psi =$ air gap flux linkage $= l_{ad} i_{fr}$

The eqn. (6) can be rewritten as

$$v'_{qs} = (v_{qs} - \omega_r \Psi) = r_a i_{qs} + l_{qs} p i_{qs} + l_{aq} p i_{qr} + \omega_r l_{ds} i_{ds} + \omega_r l_{ad} i_{dr} \quad (10)$$

The electrical torque developed is

$$T_e = \frac{3P}{2} [(l_{ad} - l_{aq}) i_{qs} i_{ds} + l_{ad} i_{qs} i_{dr} - l_{aq} i_{qr} i_{ds} + \Psi i_{qs}] \quad (11)$$

The torque balance equation is

$$\frac{2}{P} J p \omega_r = T_e - T_l - \frac{2}{P} \beta \omega_r \quad (12)$$

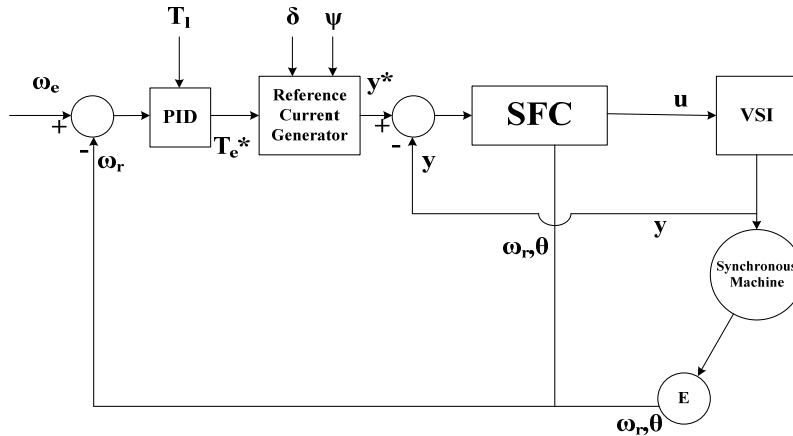


Figure-1. Block diagram representation of the proposed control scheme (Here SFC- State Feedback Controller).

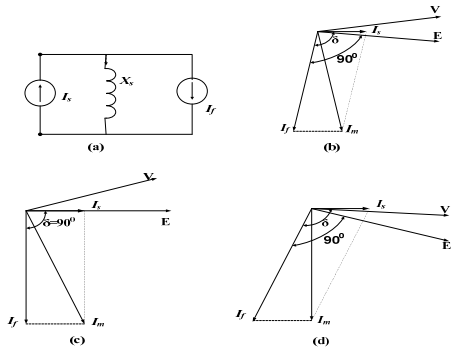


Figure-2. Equivalent circuits and Phasor diagrams of PMAC motor.

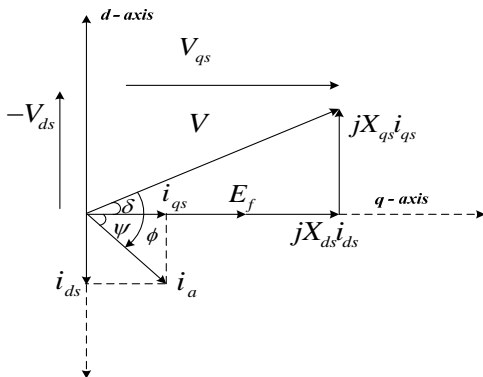


Figure-3. Phasor diagram.

Where all voltages (v) and currents (i) are refer to the rotor reference frame. The subscripts qs, ds, qr and dr correspond to q and d axis quantities for the stator(s) and rotor(r) in all combinations, r_a denotes the armature resistance, l_{qs} denotes quadrature axis inductance, l_{ds} denotes direct axis inductance etc. and T_e is the developed torque. The rotor speed is given by ω_r and the load torque by T_l , J is moment of inertia, P is the number of poles and

β is the co-efficient of viscous friction. The derivative operator is represented by the symbol p.

3. DETERMINATION OF REFERENCE CURRENTS FOR DESIRED Ψ

The generated electrical torque in equation (11) is a function of the states i.e., the stator and rotor (field and damper winding) currents of the PM synchronous motor. Since, this function is a non-linear, there are many possible values of these currents for the generation of the same torque. Thus, there is a great deal of flexibility in the choice of the reference values for these currents [2]. The following three conditions are imposed to obtain unique solution for these reference currents.

- a) The arbitrary setting of internal angle, ψ .
- b) The arbitrary setting of torque angle, δ
- c) All the reference currents should be real valued.

The phasor diagram of salient pole synchronous motor is shown in fig 3. Referring to the phasor diagram

$$\tan \delta = \frac{-v_{ds}}{v_{qs}} \tag{13}$$

Substituting v_{qs} and v_{ds} values in equation (13)

$$\tan \delta = \frac{-r_a i_{ds} - l_{ds} p i_{ds} - l_{ad} p i_{ds} + \omega_r l_{qs} i_{qs} + \omega_r i_{aq} i_{qr}}{r_a i_{qs} + l_{qs} p i_{qs} + l_{aq} p i_{qr} + \omega_r l_{ds} i_{ds} + \omega_r l_{ad} i_{dr} + \omega_r \Psi}$$

Under steady state condition with all p or $\frac{d}{dt}$ terms as well as i_{dr} and i_{qr} assumed to be zero, we get

$$\tan \delta = \frac{\omega_r l_{qs} i_{qs} - r_a i_{ds}}{r_a i_{qs} + \omega_r l_{ds} i_{ds} + \omega_r \Psi} \tag{14}$$

(i) Taking ψ as a specification



From the above phasor diagram

$$i_{ds} = i_{qs} \tan \psi \quad (15)$$

The torque equation of a PMSM is given by

$$T_e = \frac{3P}{2} [(l_{ad} - l_{aq})i_{ds}i_{qs} + l_{ad}i_{qs}i_{dr} - l_{aq}i_{qr}i_{ds} + \Psi i_{qs}]$$

Also the steady state torque from the above equation for number of poles, P=4

$$T_e = 3 [(l_{ad} - l_{aq})i_{ds}i_{qs} + \Psi i_{qs}] \quad (16)$$

On substituting equation (15) in equation (16), we have

$$T_e = 3(l_{ad} - l_{aq})i_{qs}^2 \tan \psi + 3\Psi i_{qs} \quad (17)$$

Therefore, the roots of the above equation can be obtained

$$\text{as } i_{qs}^* = \frac{-3\Psi \pm \sqrt{9\Psi^2 + 12T_e^*(l_{ad} - l_{aq})\tan \psi}}{6(l_{ad} - l_{aq})\tan \psi} \quad (18)$$

The value of i_{ds}^* is obtained by substituting the value of i_{qs}^* from equation (18) in equation (15). The power factor of a permanent magnet motor is varied from lagging to leading through unity by setting ψ from a positive to negative value through zero.

(ii) Field oriented control (FOC)

In PMSM field oriented control can be achieved by setting $\psi=0$ in equation (15). Therefore the reference currents i_{ds}^* is given by

$$i_{ds}^* = 0 \quad (19)$$

Substituting equation(19) in equation (16), the reference torque is obtained as,

$$T_e^* = 3\Psi i_{qs}^*$$

$$\text{or } i_{qs}^* = \frac{T_e^*}{3\Psi} \quad (20)$$

Field oriented control can be obtained for a value of δ permissible with a range depending upon the design consideration of a motor. Thus referring back to the phasor diagram of Figure-3 by a variable ψ the power factor angle ϕ could be varied directly. However the motor runs always at a lagging power factor in field oriented control.

4. DESIGN STRATEGIES

The design methodology for the speed controller as outlined in the previous sections, allows one to choose ψ or δ or both of them independently in order to meet a certain control objective, such as unity power factor, field orientation etc. But, there is scope for more general types of control, which can have useful engineering implications.

In this section, the above design specifications are, therefore, being viewed from this perspective.

A synchronous motor is a doubly excited machine; its armature winding is energized from an inverter and its field winding from a dc source. When synchronous motor is working at constant applied voltage, the resultant air gap flux as demanded by constant terminal voltage remains substantially constant. This resultant air gap flux is established by the co-operation of both ac in the armature winding and dc in the field winding. If the field current is sufficient enough to set up the air gap flux, as demanded by constant V then magnetizing current or lagging reactive volt ampere required from the AC source is zero and therefore, the motor operates at unity power factor. This field current which causes unity power factor operation of the synchronous motor is called normal excitation or normal field current.

If the field excitation E_f is made less than the normal excitation, i.e. the motor is under excited then the deficiency in the flux (=constant air gap flux –flux setup by dc in the field winding) must be made up by the armature winding. In order to do the needful, the armature winding draws a magnetizing current or lagging reactive volt ampere from the ac source and as a result of it, the motor operates at a lagging power factor. In case the field is made more than its normal excitation, i.e. the motor is over excited, then the excess flux (=flux setup by dc in the field winding–resultant air gap flux) must be neutralized by the armature winding. The armature can do so only if it draws a demagnetizing component current from the ac source. Since in a motor, the magnetizing current lags the applied voltage by about 90° , the demagnetizing component of current must lead the applied voltage by about 90° . In view of this, the excess flux can be counter balanced only if the armature takes a demagnetizing current or leading reactive Volt Ampere from the ac source; consequently the synchronous motor operates at a leading power factor.

A laboratory scale PMSM with a damper winding is taken up as case study. The rating of the machine as well as the values of the parameters is given in the Appendix. Let us first consider a constant flux case. This corresponds to the case of a permanent magnet motor. For the motor considered here, we set the value of i_{fr}^* to be 1A. Then for different values of T_e^* , we can obtain the characteristics of i_{qs}^* and i_{ds}^* as a function of ψ as shown in fig.4, which represents a family of characteristics of armature currents and power factor angle as a function of the specification ψ for different values of T_e^* and constant $\Psi = 1.0\text{Wb}$. From these currents, we can compute the r.m.s. currents per phase as well as the power factor for given values of ψ and T_e^* .

For a motor the reactive power is given by

$$Q = \frac{V}{X_s} (V - E_f \cos \delta) \quad (21)$$



Also, from vector diagram of Figure-3

$$\delta + \psi = \phi \quad (22)$$

The reactive power given in equation (21) is of interest only at the input terminal of the motor. It is observed from the curves as shown in Figure-4.

5. RESULTS AND DISCUSSIONS

- a) Figure-2 indicates the performance Figures for PMAC motor as a function of ψ and variable T_e . It is observed from Tables-2 & 3 and from Figures-4(d) & 5(d) that the upf value occurs at around -62.5° with i_{phase} as almost 10A, which clearly indicates that it is an absurd value as it is too high compared with rated specifications of the motor.
- b) The range of ψ is -65° to 80° as per design guidelines but the working range of the motor through simulation is -45° to 62° .
- c) It is inherent from equation (18) that δ is inversely proportional to ψ . From Table-2 and Figure-4 it is observed that upf occurs at $\psi = -12.08^\circ$.
- d) For values of ψ increasing from -45° to -12.08° δ decreases, and $\cos\delta$ increases, therefore $E_f \cos\delta > V$, which depicts the motor delivering reactive power to the mains and is operating at a leading power factor, which is clear from Table-1 (i.e., $\psi = -45^\circ$) the achieved ϕ is negative and equal to -16.40° , indicating leading power factor.
- e) From vector diagram of Figure-3, when $\psi = 0^\circ$, $i_{ds} = 0$ and the power factor angle, $\phi = \text{torque angle}$, δ and this is point of FOC, which means that the total current i_{phase} is equal to i_{qs} and is only magnetizing, which is depicted from Figure-4(a), 4(b) & 4(c). Hence motor supplies reactive power to the lines, and the power factor angle $\phi = \delta = 8.77^\circ$ and the power factor is 0.79 and is found to be always a lagging one, depicted from the Figure-4(d).
- f) For values of ψ decreasing from 62° to -12.08° , $E_f \cos\delta < V$ which is an under excited condition where Q is positive that means the motor absorbing reactive power from the mains and is operating at a lagging power factor, which is clear from Figure-4(d) in the plot of power factor angle ϕ versus ψ , the power factor angle ϕ is positive and thus lagging. As the ψ increases, then current increases gradually to a maximum value of $i_{\text{phase}} = 9.68\text{A}$ at $\psi = 62.115^\circ$.
- g) For lower values of flux say 0, 0.1, 0.2, 0.5 Wb/pole etc, power factor angle ϕ is observed to be always leading and not reaching to upf($\phi = 0^\circ$) or leading as ψ is increasing, except for flux= 1.0 Wb/pole (Figure-5.d)
- h) At $\psi = -12.567^\circ$ motor operates with upf and from ψ varying from -45.0° to -12.567° works with leading p.f and beyond which i.e., ψ varying from -12.567° to 60.0° motor works with lagging pf.
- i) In Table-3 and Figure-5(c), i_{phase} is totally administered by the flux component of armature current i.e., i_{ds} . Moreover i_{ds} and i_{qs} balances in a very amicable way to give that type of the nature of curve for i_{phase} shown in Figure-5(c) and the minimum point of i_{phase} observed is almost constant for certain values (-40° to 50°) of ψ which gives the minimum resultant power of the motor and the minimum point of i_{phase} observed is around 3.08 amps at $\psi = 10.0^\circ$ as shown in Table-2
- j) It is observed from Figures-4(c) & 5(c) that i_{phase} is administered by i_{qs} for lower values of ψ and by i_{ds} for higher values of ψ . This transition occurs at $\psi = 45^\circ$ ($i_{ds} = i_{qs} = 2.824\text{A}$) which is clearly shown in Table-2.
- k) At $\psi = -65.25^\circ$, we observe a second upf, but the armature current observed is $i_{\text{phase}} = 9.91\text{A}$ which is absurd when compared to the output specifications of the motor.
- l) It is observed in Figure-5(d) that power factor angle curves intersect at $\psi = 36.23^\circ$ for all values flux, which means for different values of flux (say 0, 0.5 & 1.0Wb/pole) the power factor remains the same. At $\psi = 36.23^\circ$ as flux is decreased from 1 to 0Wb/pole the i_{phase} is increasing rapidly, meaning that the machine is absorbing more current to compensate the weakened flux and hence operates in lagging power factor (from Table 3). As ψ is increasing, for lower values of flux, pf angle ϕ is lagging and for higher values of flux the pf angle ϕ is leading.
- m) From Figure-4(b), we observe that the curves meet at $\psi = 0^\circ$, since $i_{ds} = 0\text{A}$ at FOC, whatever may be the value of the torque.

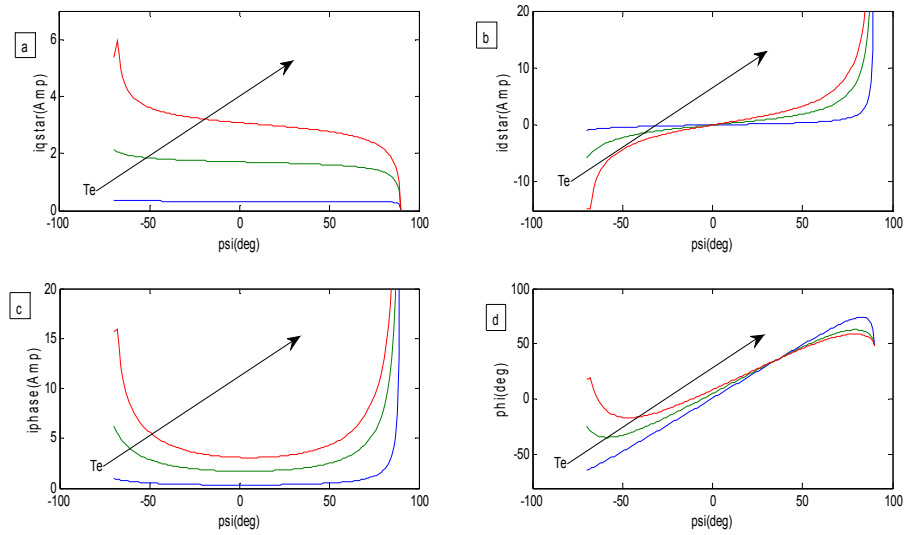


Figure-4. Family of characteristics of armature currents and power factor angle as a function of ψ for different values of T_e .

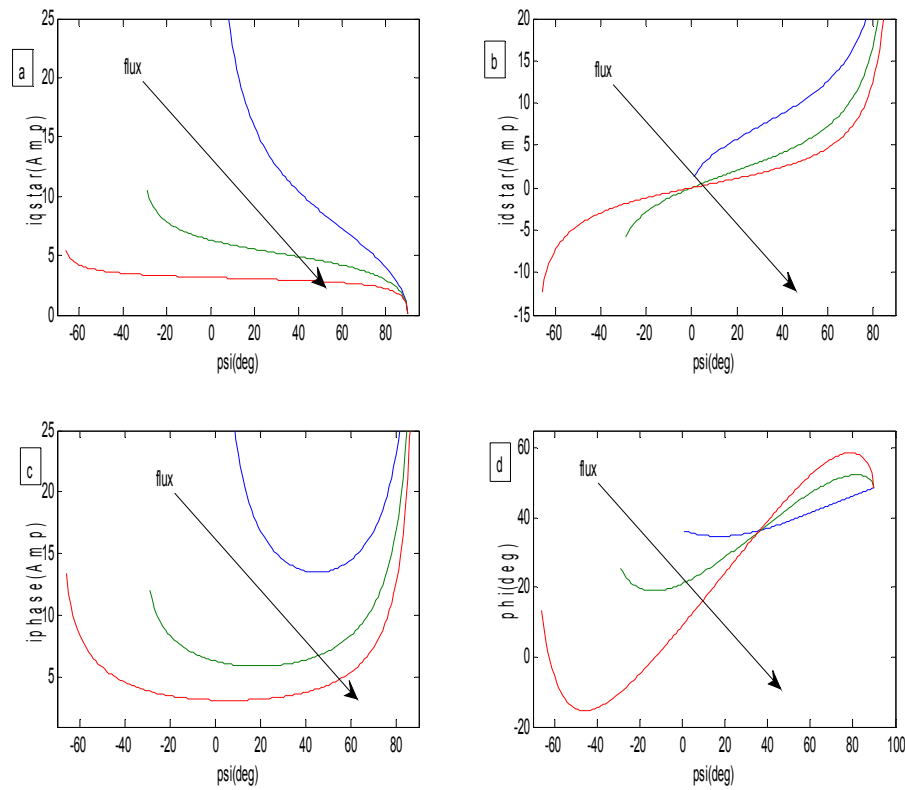


Figure-5. Family of characteristics of armature currents and power factor for as a function of ψ for different values of flux.

**Table-1.** Performance figures for PMAC motor as a function of ψ and variable T_e (D=Design Guidelines, S= Simulation results).

Design specifications, ψ	Achieved values of									
	δ through h	ϕ through		$\cos\phi$ through h	i_{qs}		i_{ds}		i_{phase}	
Set value	S	D	S	S	D	S	D	S	D	S
-45 (max lead)	28.6	-16.4	-16.39	-0.78	3.52	3.51	-3.51	-3.51	4.97	4.97
-25 (random lead)	16.56	-8.44	-8.44	-0.55	3.27	3.27	-1.52	-1.52	3.6	3.6
-15 (middle lead)	12.98	-2.02	-2.02	-0.43	3.19	3.18	-0.85	-0.85	3.3	3.3
-12.1(min lead)	12.08	-0.017	-0.016	0.99	3.17	3.169	-0.68	-0.68	3.24	3.241
-12.07 (upf)	12.07	0	0	1	3.17	3.17	-0.68	-0.68	3.24	3.24
-12 (min lag)	12.054	0.05	0.054	0.99	3.17	3.168	-0.673	-0.67	3.23	3.23
-1 (middle lag)	9.02	8.019	8.02	-0.166	3.101	3.1	-0.05	-0.05	3.101	3.1
0 (FOC)	8.77	8.77	8.77	-0.79	3.097	3.096	0	0	3.097	3.09
1 (random lag)	8.51	9.51	9.51	-0.99	3.09	3.09	0.053	0.054	3.09	3.09
45	-2.45	42.55	42.55	0.134	2.82	2.83	2.82	2.83	3.99	3.99
62 (max lag)	-8.72	53.3	53.29	-0.99	2.65	2.65	4.98	4.99	5.64	5.64

Table-2. Performance figures for PMAC motor as a function of ψ and variable T_e - only design values.

Range of ψ for T_e variable (-65° to 80°)	ϕ	$\cos\phi$	i_{qs}		i_{phase}
-65	4.99	0.279	4.71	-10.11	11.15
-63.4589 (upf value)	0	1	4.43	-8.86	9.91
-40 (max lead)	-15.439	-0.964	3.43	-2.87	4.479
-30	-11.242	0.244	3.31	-1.911	3.82
-20 (middle lead)	-5.34	0.587	3.22	-1.17	3.43
-12.1 (min lead)	-0.01	0.999	3.16	-0.679	3.24
-12.08 (upf value)	0	1.00 (upf)	3.16	-0.67	3.24
-12 (min lag)	0.0541	0.998	3.168	-0.673	3.23
-5	5.07	0.35	3.125	-0.22	3.137
(FOC) 0 ($T_e = 9.445$)	8.764	-0.79	3.09	0	3.09
($T_e=4.2225$)	8.764	-0.79	1.71	0	1.71
($T_e=1$)	8.764	-0.79	0.33	0	0.33
10	16.326	-0.815	3.04	0.536	3.087
25 (middle lag)	27.79	-0.888	2.957	1.37	3.26
36.223 ($T_e = 9.445$)	36.223	0.107	2.8883	2.1157	3.5803
($T_e=4.2225$)	36.223	0.106	1.6445	1.2046	2.0385
($T_e=1$)	36.223	0.105	0.3251	0.2382	0.403
45	42.547	0.1359	2.824	2.824	3.99
60 (max lag)	52.21	-0.368	2.67	4.62	5.34
80(absurd)	58.78	-0.616	2.18	12.36	12.56

**Table-3.** Performance figures for PMAC motor as a function of ψ with variable flux- only design values.

Range of delta for flux variable (-65° to 80°)	ϕ	$\cos\phi$	i_{qs}	i_{ds}	i_{phase}
-65	8.21	-0.3483	4.99	-10.72	11.83
-62.5235	0	1	4.48	-8.62	9.72
-60	-5.578	0.995	4.21	-7.29	8.41
-25	-7.94	0.99	3.32	-1.55	3.67
-12.567 (upf)	0	1	3.2286	-0.7197	3.3078
-5	5.34	0.99	3.17	-0.27	3.19
0(FOC)	8.99	0.98	3.14	0.0 (FOC)	3.14
10	16.48	0.958	3.09	0.54	3.13
30	31.62	0.851	2.97	1.71	3.43
36.23 at flux=0	36.23	0.1038	11.15	8.1734	13.83
36.23 at flux = 0.5	36.23	0.1029	5.02	3.6	6.228
36.23 at flux = 1	36.23	1.022	2.93	2.15	3.63
60	52.064	0.614	2.7	4.69	5.41
80	58.57	0.521	2.2	12.47	12.67

6. CONCLUSIONS

In this paper a generalized approach to the design for the torque angle control of a nonlinear vector controller of Sinusoidal PMAC Motor has been presented. It is found that, by the variation of internal power factor angle ψ there is a wide range of dynamic performance. This also gives rise to the flexibility of choosing the pf from lagging to leading through unity. Field Oriented Control is also obtained as a special case by choosing the internal power factor angle (ψ) to be zero. This result in complete decoupling between the armature and field flux, allowing them to be controlled independently, like a dc motor improving the dynamic performance of the system.

APPENDIX: Machine Rating and Parameters of Permanent Magnet Synchronous Motor (PMSM) [2]

Stator: 400 V, 2.17A, 3- ϕ 50Hz, 1500rpm, 4-pole

Rotor or Field: 85 V, 1.6 A, DC, Salient Pole.

Performing the various tests in the laboratory, parameters of the synchronous motor are found as,

$r_a=5.5\Omega$, $r_{dr}=16.0\Omega$, $r_{qr}=4.2\Omega$, $r_{fr}=0.31\Omega$, $l_f=0.016H$, $l_{ad}=0.048H$, $l_{fr}=0.092H$, $l_{dr}=0.14H$, $l_{qr}=0.14H$, $\beta=0.0049N.m/sec/rad$, $J=0.048kg.m^2$.

REFERENCES

- [1] K. Alice Mary, A. Patra. and N. K. De. 2007. A Generalized Approach to the Design of the Speed Control system for Inverter-Driven Permanent Magnet Synchronous Motor. IET-UK International Conference on Information and Communication Technology in Electrical Sciences, Tamil Nadu, December, pp. 20-22.
- [2] K. Alice Mary, A. Patra, N.K. De. and S. Sengupta. 2002. Design and implementation of the Control system for Inverter-fed Synchronous Motor drive. IEEE Transactions on Control Systems Technology. Vol. 10, No. 6, November, pp.853-859.
- [3] G. K. Dubey. 1995. Fundamentals of electrical drives. Narosa Publications, 1st edition.
- [4] P. Ramana, B. Santhosh Kumar, K. Alice Mary. and M. Surya Kalavathi. 2013. Comparison of Various PWM Techniques for Field Oriented Control VSI fed PMSM Drive. International Journal of Advanced Research in Electrical, Electronics and Instrumentation Engineering. Vol.2, Issue-7, July, pp. 2928-2936.
- [5] F. Heydari, A. Sheikholeslami, K. G. Firouzjeh. and S. Lesan. 2010. Predictive field-oriented control of PMSM with space vector modulation technique," Front. Electrical Electronics Engineering. Vol.5, Issue.1, China, pp. 91-99.
- [6] Hasni Mourad, Touhami Omar, Ibtien Rachid, M. Fadeland. and Stephane Caux. 2010. Modelling. and Parameter Identification of Synchronous Machine by PWM Excitation Signals. IEEE International Symposium on Power Electronics, Electrical Drives, Automation and Motion, pp. 442-447.
- [7] Basar Bech M. M., Andersen T.O., Scavenius P. and Thomas-Basar T. 2013. Comparison of sensorless FOC and SVM-DTFC of PMSM for low-speed applications," 4th international Conference on Power Engineering, Energy and Electrical Drives, May-Istanbul, pp. 864-869.